Ultrasonics - Sonochemistry 66 (2020) 105043

Contents lists available at ScienceDirect

Ultrasonics - Sonochemistry

journal homepage: www.elsevier.com/locate/ultson

One-pot sonochemical synthesis of CuS nanoplates decorated partially reduced graphene oxide for biosensing of dopamine neurotransmitter

Selvakumar Palanisamy[a,*], Sethupathi Velmurugan[b], Thomas C.K. Yang[a,b,*]

[a] Center of Precision Analysis and Material Research, National Taipei University of Technology, No. 1, Section 3, Chung-Hsiao East Road, Taipei 106, Taiwan, ROC
[b] Department of Chemical Engineering and Biotechnology, National Taipei University of Technology, No. 1, Section 3, Chung-Hsiao East Road, Taipei 106, Taiwan, ROC

ARTICLE INFO

Keywords:
Sonochemical synthesis
Partially reduced graphene oxide
Neurotransmitter
CuS nanoplates
Biosensor

ABSTRACT

The sonochemical methods have been used as a straight forward method for the synthesis of various composite materials, including the transition metal dichalcogenide composites. In the present work, we report a simple sonochemical synthesis of CuS nanoplates decorated partially reduced graphene oxide (PrGO) nanocomposite for the first time. The PrGO-CuS nanocomposite was synthesized using bath-sonication (frequency: 37 kHz; power: 150 W) of graphene oxide (GO), and CuS precursors at 80 °C for 60 min. The physicochemical characterization (FESEM, XRD, FTIR, and Raman spectroscopy) results confirmed the successful formation of CuS nanoplates on PrGO nanosheets. The as-synthesized PrGO-CuS nanocomposite was further utilized for electroanalysis of dopamine neurotransmitter. The obtained electroanalytical results revealed that PrGO-CuS nanocomposite has superior electrochemical activity towards dopamine than those obtained for GO, CuS, and GO-CuS composite. The fabricated biosensor shows a lower limit of detection (0.022 μM) with a more comprehensive linear response range (0.1–155.1 μM) for the detection of dopamine. Moreover, the PrGO-CuS nanocomposite electrode was successfully used for the detection of dopamine in bovine serum albumin.

1. Introduction

The derivatives of graphene oxide composite materials have been attracted to various potential applications, including energy devices and photovoltaic and biosensor applications [1–3]. Among them, the reduced graphene oxide or partially reduced graphene oxide (PrGO) has received tremendous interest due to its auspicious 2D nature along with specific unique properties, such as more substantial surface area, excellent electrochemical and thermal conductivity, chemical inertness and high stability [4,5]. Nevertheless, the direct use of PrGO in electroanalytical applications is limited due to its re-stacking of PrGO layers to graphite for extended time use [6]. Therefore, the composites of PrGO has been used as an alternative to prolong the unique properties of PrGO and preventing the re-stacking of PrGO [7]. In recent years, the range of PrGO composites has been synthesized by numerous methods, which include the chemical, sonochemical, thermal, and electrochemical methods [8–11]. For instance, the metal dichalcogenides (CuS, MoS_2, and SnS_2), metal alloy/oxide nanoparticles (Au, Zn, Pt, Pd, and Cu) and carbon nanomaterials (carbon nanotubes and C60) have been predominantly used as support for the synthesis of PrGO composites [9,12–17]. Among them, the covellite copper sulfide (CuS) is well known binary inorganic semiconductor material (bandgap of 1.21 eV), has shown considerable attention in various fields, including solar cells, photodetectors, photocatalysis, gas sensors, and electrochemical sensors [18]. The CuS nanostructures have been synthesized using different methods such as hydrothermal/solvothermal method, electrodeposition, and sonochemical and or solution-based methods [18–20]. In comparison with other methods, the sonochemical synthesis of CuS is found as an efficient and straightforward route due to its simplicity and prolong reaction conditions [9,20]. Also, the sonochemical method is an excellent choice for the one-pot simultaneous preparation of CuS and PrGO using CuS and PrGO precursors at 80 °C since this method does not need specific templates, toxic reagents, and higher temperatures.

Dopamine is an essential neurotransmitter and is mainly responsible for the neurological and psychiatric disorders, and the dysfunctions of dopamine in the central nervous system lead to Parkinson's disease, and schizophrenia [21]. Henceforth, the real-time monitoring of dopamine levels in biological samples is essential and clinically significant. Compared to available methods, the dopamine can be easily detected using the electrochemical methods since it is highly active on the unmodified carbon electrodes [22–24]. Over the past decades, the composites of PrGO have mainly been used as an electrode material for the

* Corresponding authors at: Center of Precision Analysis and Material Research, National Taipei University of Technology, No. 1, Section 3, Chung-Hsiao East Road, Taipei 106, Taiwan, ROC (S. Palanisamy; T.C.K. Yang).
E-mail addresses: prmselva@gmail.com (S. Palanisamy), ckyang@mail.ntut.edu.tw (T.C.K. Yang).

https://doi.org/10.1016/j.ultsonch.2020.105043
Received 31 January 2020; Received in revised form 19 February 2020; Accepted 21 February 2020
Available online 22 February 2020
1350-4177/

construction of dopamine biosensors, and they have shown improved sensitivity and limit of detection (LoD) along with high selectivity towards dopamine than pristine PrGO and unmodified carbon electrodes [25–27]. However, in the present work, we have used PrGO-CuS nanocomposite as a selective electrode material for the fabrication of real-time dopamine biosensor. The PrGO-CuS nanocomposite was synthesized for the first time using the one-pot sonochemical method. The electrocatalytic redox behaviors of dopamine on PrGO-CuS nanocomposite have been studied comprehensively and compared with GO, CuS, GO-CuS modified electrodes using cyclic voltammetry (CV). The limit of quantitation (LoQ) and the LoD of the fabricated sensor electrode was also estimated.

2. Experimental section

2.1. Materials & methods

The raw graphite powder (average particle size of about less than 20 μM) was purchased from Sigma-Aldrich. Dopamine hydrochloride powder and thiourea (ACS reagent, ≥99.0%) were obtained from MERCH, Taiwan. Cupric nitrate trihydrate ($Cu(NO_3)_2{\cdot}3H_2O$) was received from the CHONEYE PURE CHEMICALS, Taiwan. All the interfering compounds tested in this work were purchased from the Sigma-Aldrich Company, Taiwan. The bovine serum albumin (BSA) solution was received from Sigma-Aldrich and was used as received without any pretreatment process. The S-4000 sonicator from Misonix, Inc (frequency: 37 kHz; maximum operating power: 150 W)) was used for the sonochemical synthesis of nanomaterials. The XPERT-PRO XRD from PANalytical B.V. was used to acquiring the XRD of the as-synthesized materials. The JEOL JSM-7610F high-resolution field emission scanning electron microscope (FESEM) was used for acquiring the surface scanning images of the materials. The energy dispersive X-ray (EDX) spectroscopy and elemental mapping of the nanocomposite were obtained using EDX analyzer attached JEOL JSM-7610F high-resolution FESEM from the Oxford Instruments. The CHI-1211c electrochemical analyzer with standard three-electrode configuration was used for the electroanalytical applications. The electroanalytical studies were performed using 0.05 M phosphate buffer (pH 7.0) and were adjusted to other pHs using either 0.1 M NaOH or 0.1 M sulphuric acid. The de-ionized water was used as a solvent for all chemicals in the synthesis part.

2.2. Sonochemical synthesis of PrGO-CuS nanocomposite

The graphite oxide (synthesized using the Hummers' method) was sonochemically exfoliated into the graphene oxide (GO) [28], where the graphite oxide (2 mg/mL) was dispersed into the water using the bath-sonication method (frequency: 37 kHz; power: 150 W) for 30 min. Then, about 5 mM of $Cu(NO_3)_2{\cdot}3H_2O$ was added to the GO dispersion and bath-sonicated for 5 min at room temperature. About 0.5 M of thiourea was added into the GO-Cu precursor solution, and the temperature of the bath was maintained at 80 °C. Herein, the thiourea was used for the source of sulfide with GO-Cu precursor solution. The above mixture was continuously bath-sonicated for 60 min with a maximum frequency and power output. After the sonochemical reaction, the black precipitate of PrGO-CuS nanocomposite was obtained and was washed with ice-cold water and centrifuged at 5000 RPM. The final obtained PrGO-CuS nanocomposite was dried at 50 °C for further use. Likewise, the CuS was prepared using the sonochemical method mentioned above without GO. For comparison, the GO-CuS nanocomposite also prepared by the sonochemical method at room temperature (see Scheme 1). The detailed sonochemical synthesis procedure of PrGO-CuS nanocomposite is shown in Scheme 1. Before the electrode modifications, the glassy carbon electrode (GCE) was polished with alumina slurry using a polishing kit and washed with de-ionized water and bath-sonicated for 30 s. For electrode preparations, 2 mg/mL of PrGO-CuS nanocomposite (ethanol dispersion) and 2 mg/mL of CuS was used. About 6 μL of PrGO-CuS nanocomposite and 3 μL of CuS and GO coated GCEs were used for the electroanalytical studies.

3. Results and discussions

3.1. Characterizations

The XRD, FTIR, and Raman spectroscopy were employed to verify the formation of PrGO-CuS nanocomposite and amble reduction of GO to PrGO. As shown in Fig. 1A, the FTIR spectrum of GO (curve a) shows characteristic vibration bands for the presence of −OH (3150–3630 cm^{-1}), C═O (1728 cm^{-1}), C−OH (1628 cm^{-1}), C−O−C (1381 cm^{-1}), and C−OH (1052 cm^{-1}), which reveals the successful oxidation of graphite [6]. The FTIR spectrum of pristine CuS (curve b) shows an active vibration band related to Cu−S was observed at 620 cm^{-1}, which confirmed the successful sonochemical synthesis of CuS. On the other hand, the vibration bands related to −OH at 3150–3630 cm^{-1} range significantly reduced upon sonochemical preparation of PrGO-CuS nanocomposite (curve c). Also, the band related to Cu-S was observed at 620 cm^{-1}, which further confirmed the formation of PrGO-CuS nanocomposite. Fig. 1B displays the typical XRD pattern of GO (a), PrGO-CuS nanocomposite (b), and CuS (c). The observed diffraction 2θ peaks of pristine CuS are well-matched with the JCPDS no. 06-0464 for the hexagonal phase of covellite CuS. Also, the sonochemically synthesized CuS has shown the dominant crystal faces as (1 1 0), (1 0 2), (1 0 3), (1 0 6) and (0 0 6) planes and were confirmed from high-intensity phenomenon (47.87°, 27.81°, 29.27°, 31.87°, 32.88°) of the 2θ peaks on the XRD pattern. The average crystalline size (Dp) of CuS on the PrGO-CuS nanocomposite composite was calculated as 21.5 nm using the Scherrer equation. A sharp diffraction peak at 2θ = 11.28° was observed in the XRD pattern of GO, which is attributed to the [0 0 1] reflections of GO. The [0 0 1] reflections of GO were significantly reduced on the XRD pattern of PrGO-CuS nanocomposite, which confirmed the successful transformation of GO to PrGO by the sonochemical method. The diffraction peaks related to pure CuS (JCPDS no. 06-0464) also appeared in the XRD pattern of PrGO-CuS nanocomposite, which further validates the formation of CuS on PrGO surface. To further confirm the above phenomenon, the Raman spectrum of GO, GO-CuS and PrGO-CuS nanocomposite was acquired, and the results are displayed in Fig. 1C. The GO (curve a) displays dominant D and G band peaks at 1349 and 1594 cm^{-1} and is resulting from the breathing modes (defects) and stretching of carbon atoms in the graphitic network. The G band intensity was dramatically reduced upon GO intercalated with CuS (curve b), and D and G bands were located at 1347 and 1583 cm^{-1}. The shift in the G band position of GO-CuS composite possibly due to the strong interaction between the CuS with GO nanosheets.

On the other hand, the Raman spectrum of PrGO-CuS nanocomposite (curve c) shows a similar D and G band position, and the intensity of the G band was further reduced when compared with GO. This is probably due to the removal of oxygen moieties from the edges of the GO surface. In addition to D and G bands, the PrGO-CuS and GO-CuS show a characteristic vibration of CuS at 469 cm^{-1}, which confirmed the presence of CuS on GO and PrGO. The I_D/I_G ratio of GO, PrGO-CuS, and GO-CuS was calculated as 0.96, 1.04, 1.02, respectively. The increase in the I_D/I_G ratio of rGO-CuS nanocomposite confirmed the successful reduction of GO by the sonochemical method. Also, the increase in the I_D/I_G ratio of GO-CuS composite revealed the variation of GO structure with CuS. The electrochemical properties of different modified electrodes were investigated using the standard ferrocyanide-ferricyanide system by CV. Fig. 1D shows typical CV responses of 0.1 M standard $Fe(CN)_6^{3-/4-}$ with KCl at bare, GO-CuS, CuS, and PrGO-CuS nanocomposite modified GCEs. A well-defined redox-couple related to the ferrocyanide-ferricyanide system was observed on all modified electrodes at a 100 mV/s scan rate. The peak to peak separation (ΔEp)

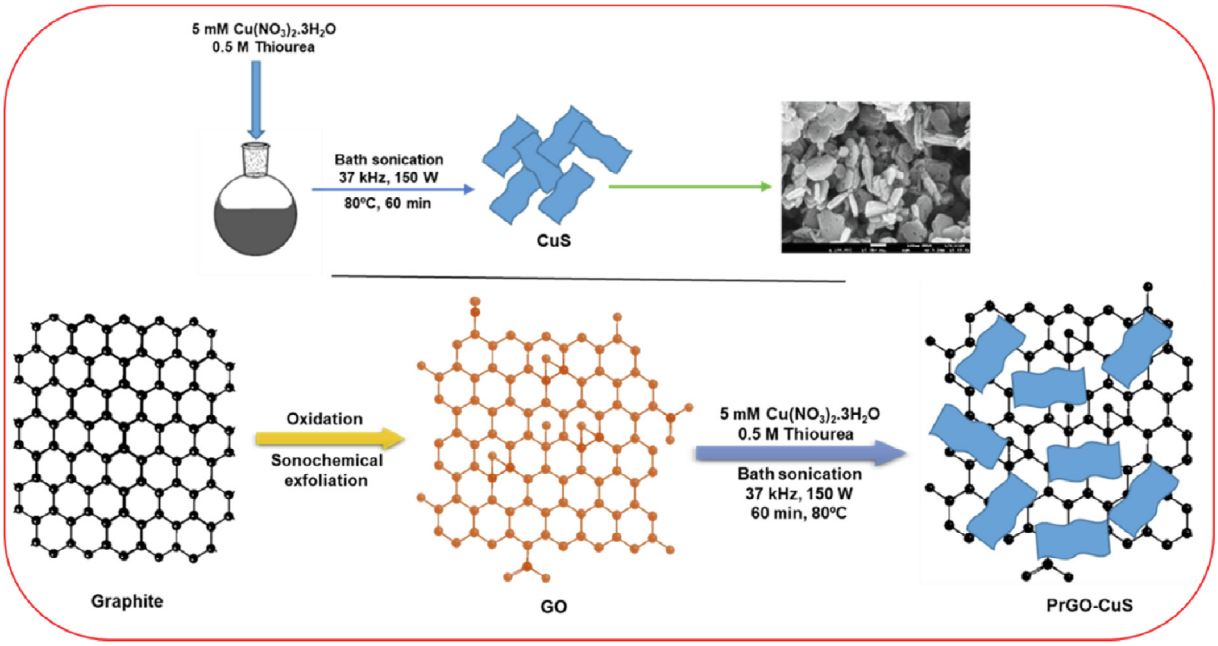

Scheme 1. The schematic illustration for the sonochemical preparation of CuS and PrGO-CuS nanocomposite.

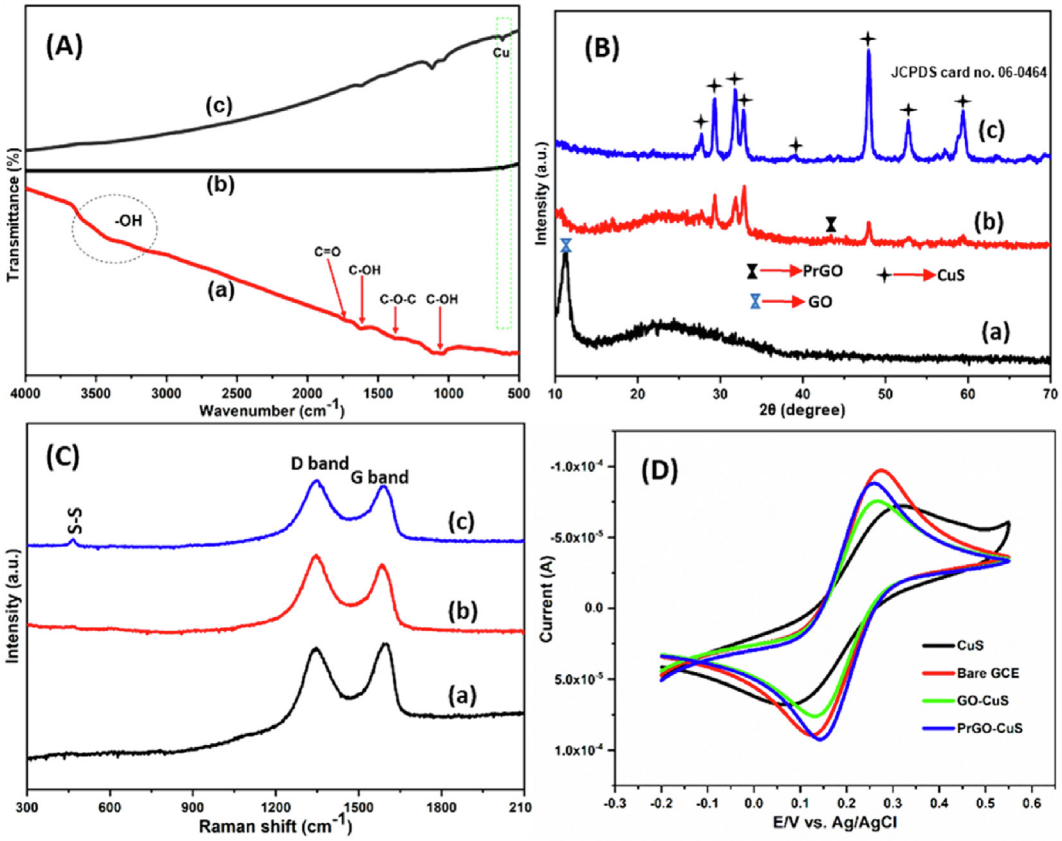

Fig. 1. A) FTIR spectra of GO (a), CuS (b), and PrGO-CuS nanocomposite (c). B) XRD pattern of GO (a), PrGO-CuS nanocomposite (b), and CuS (c). C) Raman spectra of GO (a), GO-CuS (b), and PrGO-CuS nanocomposite. D) The redox electrochemical behavior of 0.1 M $Fe(CN)_6^{3-/4-}$ on bare, GO-CuS, CuS, and PrGO-CuS nanocomposite modified GCEs.

of bare, GO-CuS, CuS, and PrGO-CuS nanocomposite modified GCEs was calculated as 136, 126, 156, and 113 mV, respectively. Also, the electron transfer ability of electrodes can be written in the order of CuS < bare < GO-CuS < PrGO-CuS, which confirmed the enhanced electron transfer ability of PrGO-CuS nanocomposite than other modified electrodes. Also, the electrochemical active surface area (EASA) of PrGO-CuS nanocomposite (0.106 cm^2) is higher than bare (0.62 cm^2), GO (0.64 cm^2) and GO-CuS (0.81 cm^2) modified electrodes. The EASA of the different electrodes were calculated using the Randles–Sevcik equation, as reported early [29]. The above results

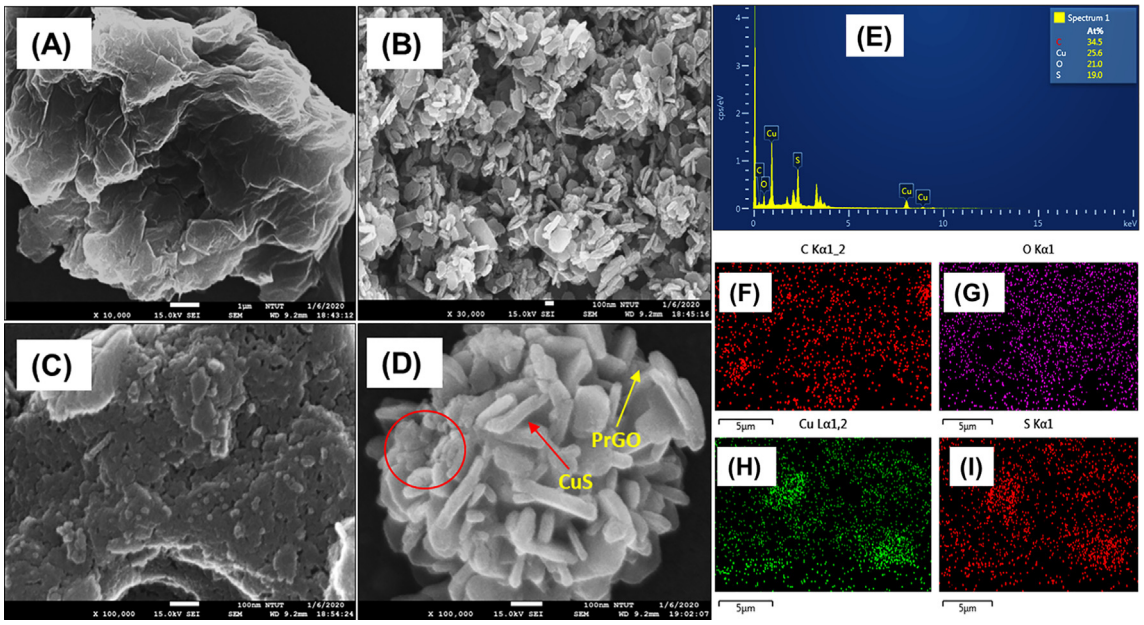

Fig. 2. High-resolution FESEM images of GO (A), CuS (B), GO-CuS (C), and PrGO-CuS (D). The EDX spectrum (E) and the corresponding elemental mapping (F-I) of sonochemically synthesized PrGO-CuS nanocomposite.

confirmed that the PrGO-CuS nanocomposite modified GCE has more EASA than other modified GCEs.

The surface morphology of sonochemically synthesized CuS, GO-CuS, and PrGO-CuS nanocomposite was investigated by FESEM, and the corresponding FESEM images are shown in Fig. 2. The FESEM image of GO (A) confirmed the structural changes of graphite into the GO nano-thin sheets. The FESEM image of CuS (B) appeared as a nano plate-like morphology with an average thickness of 26 ± 3 nm. The morphology CuS on GO (C) observed as spherical morphology where the CuS nanoparticles anchored on the ultra-thin surface of GO sheets. The above result suggests that the room temperature sonochemical synthesis of CuS does not produce sufficient activation energy to form the nanoplates; that is the reason why the CuS nanoparticles can be seen on the surface of GO. In contrast, the FESEM image of sonochemically synthesized PrGO-CuS nanocomposite (D) reveals that CuS nanoplates were anchored on the PrGO sheets, which may arise from the strong interaction between CuS and PrGO. The thickness of CuS on PrGO was found similar to sonochemically synthesized CuS, which confirmed the successful formation of PrGO-CuS nanocomposite. The EDX (Fig. 2E) confirmed the presence of carbon (34.5%), oxygen (25.6%), copper (21.0%), and sulfur (19.0%) on the PrGO-CuS nanocomposite. Also, the elemental mapping of PrGO-CuS nanocomposite is shown in Fig. 2F-I, where the carbon, oxygen, copper, and sulfur elements distribution can be seen from the selected area of the FESEM image of PrGO-CuS nanocomposite (Fig. 2D). The above characterizations confirmed that the PrGO-CuS nanocomposite could be synthesized using the sonochemical method.

3.2. Electrooxidation of dopamine

Fig. 3 shows typical CV responses obtained for the electrochemical oxidation of 10 μM dopamine on various modified GCEs at a scan rate of 50 mV/s. Typically, the electrochemical behavior of dopamine on graphene materials is quasi-reversible, where the dopamine oxidizes to dopamine o-quinone (predominant) at +0.2 to 0.4 V vs. Ag/AgCl. In our case, the GO, CuS, GO-CuS, and PrGO-CuS modified electrodes show good quasi-reversible behavior to dopamine in pH 7.0. The oxidation peak potential of dopamine was observed at 0.243, 0.206, 0.188, and 0.184 V on CuS, GO, GO-CuS, and PrGO-CuS modified GCEs. From the above, one can see that the electrode modified with PrGO-CuS

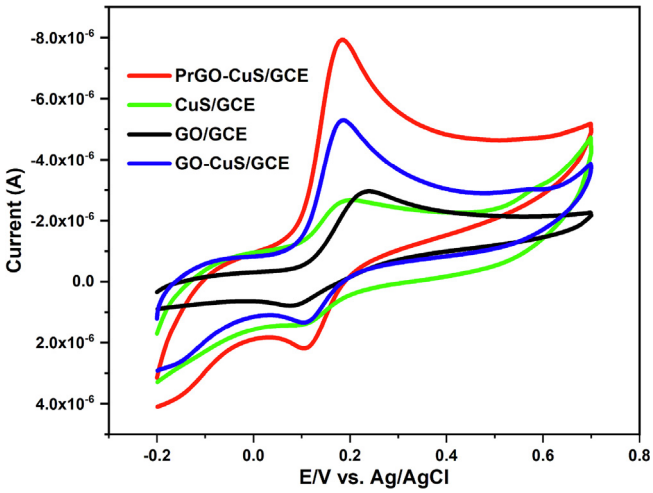

Fig. 3. CV profiles for the electrochemical oxidation and reduction of dopamine (10 μM) on GO, CuS, GO-CuS, and PrGO-CuS modified electrodes in pH 7.0 at 50 mV/s scan rate.

nanocomposite has lower oxidation peak potential and ΔEp to dopamine than other modified electrodes. The PrGO-CuS nanocomposite modified electrode has 59, 22, and 4 mV lower oxidation peak potential than CuS, GO, and GO-CuS modified electrodes. Also, the oxidation current response of dopamine on the PrGO-CuS nanocomposite was 3 and 1.3-folds higher than dopamine oxidation signal on the CuS, GO, and GO-CuS modified electrodes, respectively. The above observations confirmed the excellent electro-oxidation ability of the nanocomposite modified electrode towards dopamine, which is due to the combined synergetic activity of PrGO and CuS. The high conductivity of PrGO and excellent redox ability of CuS are resulting in the enhanced oxidation with lower potential detection of dopamine than GO and CuS. Hence, the PrGO-CuS nanocomposite could be used for sensitive biosensor for the detection of dopamine.

The effect of scan rates of the electrochemical behavior of dopamine on the nanocomposite modified electrode was investigated by CV since these studies could provide useful information about the electrochemical behavior of dopamine. The CV profiles for the effect of scan

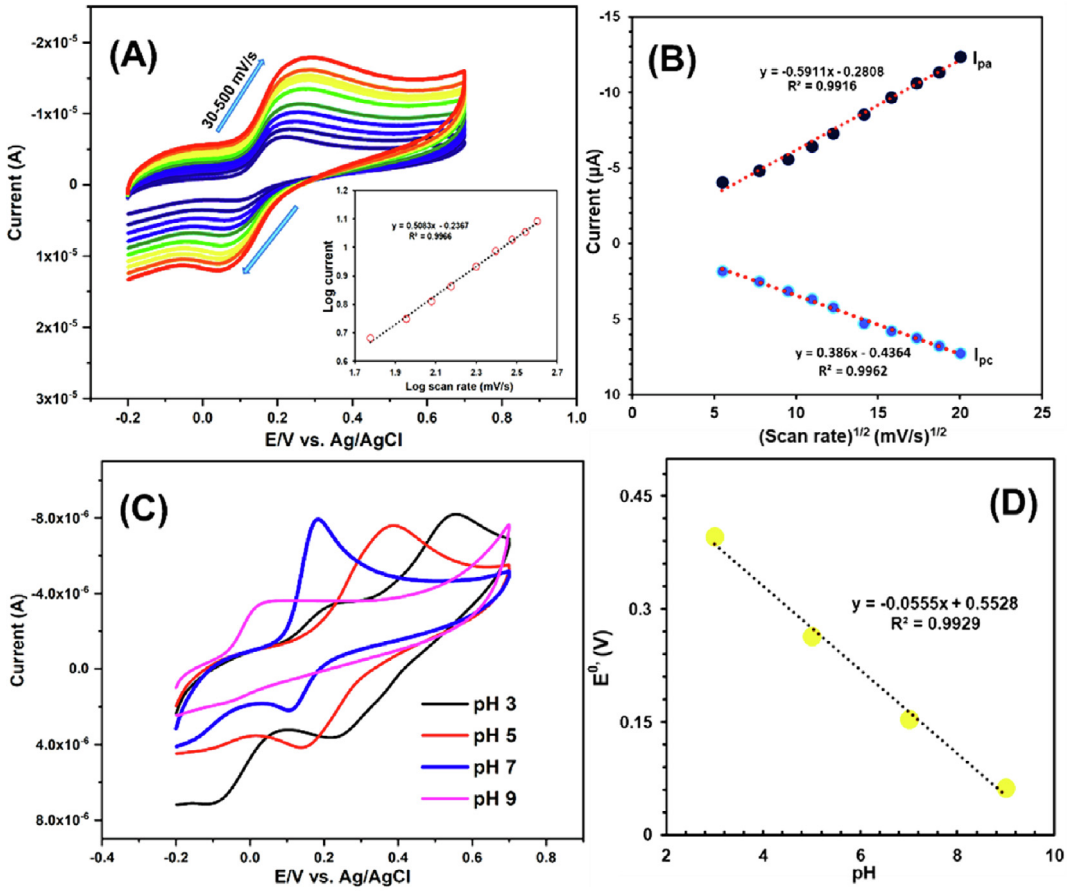

Fig. 4. A) The CV profiles for the effect of various scan rates (30–500 mV/s) on the electrochemical redox behavior of dopamine at the PrGO-CuS modified electrode. The linear plot for Log. scan rate vs. Log. current (inset of A) and the (scan rate)$^{1/2}$ vs. current (B). C) The CV curves for the effect of pH (pH 3–9) on the electrochemical redox behavior of dopamine (10 μM) on the PrGO-CuS electrode. D) The plot for the pH vs. $E^{0'}$.

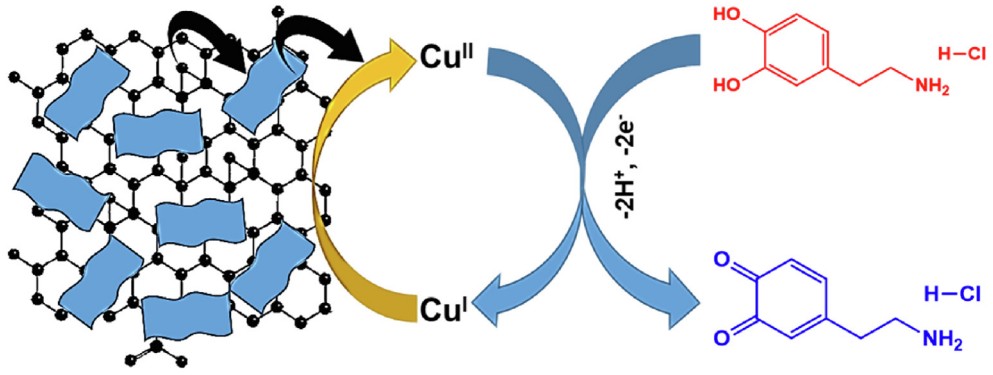

Scheme 2. The electrochemical oxidation mechanism of dopamine on PrGO-CuS nanocomposite.

rates on the electrochemical redox behavior of dopamine (10 μM in pH 7.0) at the PrGO-CuS modified electrode is shown in Fig. 4A. A well-defined quasi-redox peak of dopamine was obtained on the PrGO-CuS modified electrode for the scan rates from 30 to 500 mV/s. The oxidation and reduction peak current of dopamine increased with moderate potential shift when the scan rate was increased from lower to higher (30–500 mV/s). The redox peak current response (oxidation and reduction) of dopamine is linear to the square root of scan rates (R^2 = 0.9916 and 0.9962) as can be seen from the calibration plot of Fig. 4B. This phenomenon is called a diffusion-controlled process. To verify this phenomenon, the log current (oxidation) response of dopamine vs. log scan rate was plotted (Fig. 4A inset). The linear plot of log current dopamine vs. log scan rate gives a slope value of 0.5083. The obtained slope value confirmed that the electrooxidation of dopamine on the PrGO-CuS modified electrode is a pure diffusion-controlled process [24].

The electrochemical redox behavior of dopamine in different pH was evaluated using CV since the pH of the solution can affect the redox currents and potentials of dopamine. Fig. 4C shows the CV curves for the electrochemical redox behavior of 10 μM dopamine in various pH (pH 3–9) on the PrGO-CuS electrode. The PrGO-CuS nanocomposite shows quasi-redox behavior to dopamine in all investigated pHs (3, 5, 7, and 9). Also, the highest redox currents of dopamine were observed on pH 7 than that of pH 3, 5, and 9. Besides, Fig. 4D shows the linear relationship between the formal potential ($E^{0'}$) of DA with the pH values from 3 to 9. The obtained slope value (55.5 mV/pH) is a close

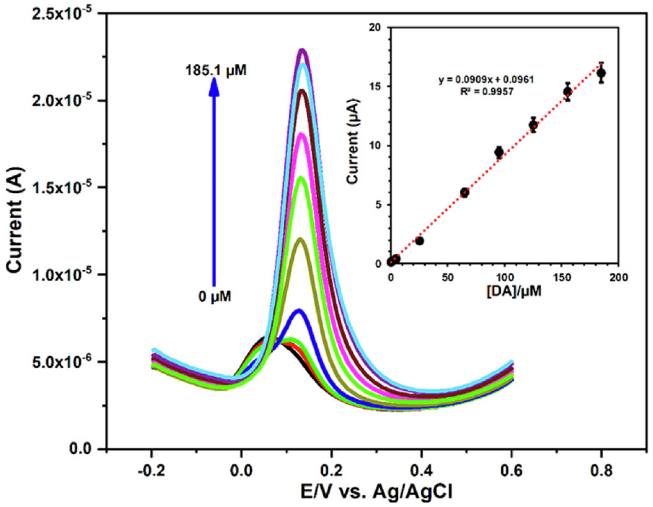

Fig. 5. DPV responses obtained on the PrGO-CuS nanocomposite modified electrode for the absence (initial curve) and the presence of dopamine (0.1–185.1 µM).

agreement with our previously reported values for two electrons, and protons transferred electrochemical redox reaction of dopamine [22–24]. The mechanism for the electro-oxidation of dopamine on PrGO-CuS nanocomposite is shown in scheme 2.

3.3. Analytical validation

The DPV was used to evaluate the analytical parameters for the detection of dopamine using the PrGO-CuS nanocomposite. Fig. 5 shows the DPV responses obtained on the PrGO-CuS nanocomposite GCE for the absence (initial curve) and the presence of dopamine (0.1–185.1 µM) in pH 7.0. In the absence of dopamine, a small anodic peak response was observed at 0.076 V and is related to oxidation of Cu^{I} to Cu^{II}. The oxidation peak related Cu^{II} was diminished upon addition of 0.1, 0.5, and 3 µM dopamine; a clear DPV signal appeared at 0.12 V. The observed DPV response at 0.12 V is due to the oxidation of dopamine (dopamine o-quinone) by the modified electrode. To further increase the addition of dopamine, the dopamine oxidation signal increases, and the signal was saturated for 185.1 µM. From the calibration plot (Fig. 5 inset), the DPV response of the modified electrode is linear from 0.1 to 155.1 µM with the sensitivity and R^2 of 0.09 µA/µL and 0.9957, respectively. The LoQ and LoD were estimated to be 26 and 22 nM, respectively. Also, it is worth mentioning that the LOD and linear response range of our sensor is more comparable to previously reported dopamine sensors, including graphene composite electrodes [22–24,30–33]. The above results revealed that the PrGO-CuS nanocomposite modified electrode can be used for sensitive and low-level detection of dopamine.

The selectivity of the sensor was also evaluated in the presence of biologically active compounds. Ascorbic acid (AA), uric acid (UA), glucose (Glu) are known human metabolites, and they could easily interfere with the dopamine response of the sensor electrode. The mixture (5 µM) of AA, UA, Glu, and acetaminophen (AC) with dopamine (0.5 µM) was examined using DPV (Fig. 6A). One can be seen from the DPV results that the interfering compound had a minimal effect (less than 5%) on the dopamine response, which is possibly due to the selective recognition of CuS towards dopamine. The result also established that the PrGO-CuS nanocomposite electrode could be used for the selective determination of dopamine. To validate the probable recognition of dopamine in biological fluids, the real sample analysis of dopamine in the bovine serum albumin (BSA) was done using fabricated nanocomposite. The known concentration of dopamine-containing BSA (100 µM) was prepared and used as a stock solution for the real sample analysis. Fig. 6B displays the DPV response obtained for the PrGO-CuS electrode for 0.1–25 µM concentration additions of dopamine-containing BSA into pH 7.0. It can be seen that the sensor electrode displays a note-worthy DPV response for the addition of 0.1, 0.5, and 3 µM dopamine-containing BSA in pH 7.0, and the obtained DPV results of dopamine (0.1–25 µM) are well-matched with Fig. 5. Therefore, the reported PrGO-CuS nanocomposite is a promising sensor platform for real-time detection of dopamine in the biological samples.

The sensor was tested for its stability and was evaluated from the signal of 0.5 µM of dopamine using DPV. The stability studies were performed using PrGO-CuS modified electrode, and the response current of dopamine was monitored from 0 to 44 h. The obtained DPV results are plotted in Fig. 6D. The stability results revealed that the PrGO-CuS modified electrode had lost 5.8 and 6.3% of its initial dopamine response for 20 and 32 h storage at 4 °C. Also, the modified electrode retains 92.9% of initial dopamine activity after the 44 h storage. The cyclic stability of the PrGO-CuS modified electrode towards the detection of dopamine was studied using CV. The modified electrode lost only 2.6% of its initial oxidation peak current to the 10 µM dopamine after 20 cycles (figure not presented). The results confirmed the adequate storage and cyclic stability of the fabricated dopamine sensor.

4. Conclusions

In conclusion, a simple sonochemical synthesis of CuS and PrGO-CuS nanocomposite has been reported and systematically characterized using various physicochemical methods. The FESEM results revealed that the CuS nanoplates were formed when the sonochemical synthesis performed at 80 °C, while CuS nanoparticles were formed at room temperature. Also, the CuS nanoplates on PrGO can be prepared using a one-pot sonochemical method at 80 °C. The XRD, FTIR, and Raman characterizations confirmed the formation of PrGO-CuS nanocomposite. The as-prepared PrGO-CuS nanocomposite modified electrode showed excellent analytical performances towards dopamine, including the acceptable linear response range (up to 155.1 µM) with lower LoD (26 nM). The fabricated dopamine sensor has good selectivity with acceptable storage and cyclic stability. The PrGO-CuS nanocomposite has also been used for the detection of dopamine in BSA, and the obtained results were satisfactory.

Author statement

S.V. synthesized and characterized the all synthesized materials. S.V. also performed electrochemical studies of dopamine sensor. P.S. prepared the figures and analyzed the data and prepared the manuscript draft. T.C.K.Y. and P.S. supervised and finalized the project. All authors discussed the results and contributed to the final manuscript.

Declaration of Competing Interest

The authors declare that they have no known competing financial interests or personal relationships that could have appeared to influence the work reported in this paper.

Acknowledgments

This project was supported by the Ministry of Science and Technology (project no. 108-2221-E-027-072) of Taiwan (Republic of China). Authors also acknowledge the Center of precision analysis and material research, National Taipei University of Technology, for providing all necessary Instrument facilities. Dr Selvakumar Palanisamy acknowledges the National Taipei University of Technology for the post-doctoral fellowship.

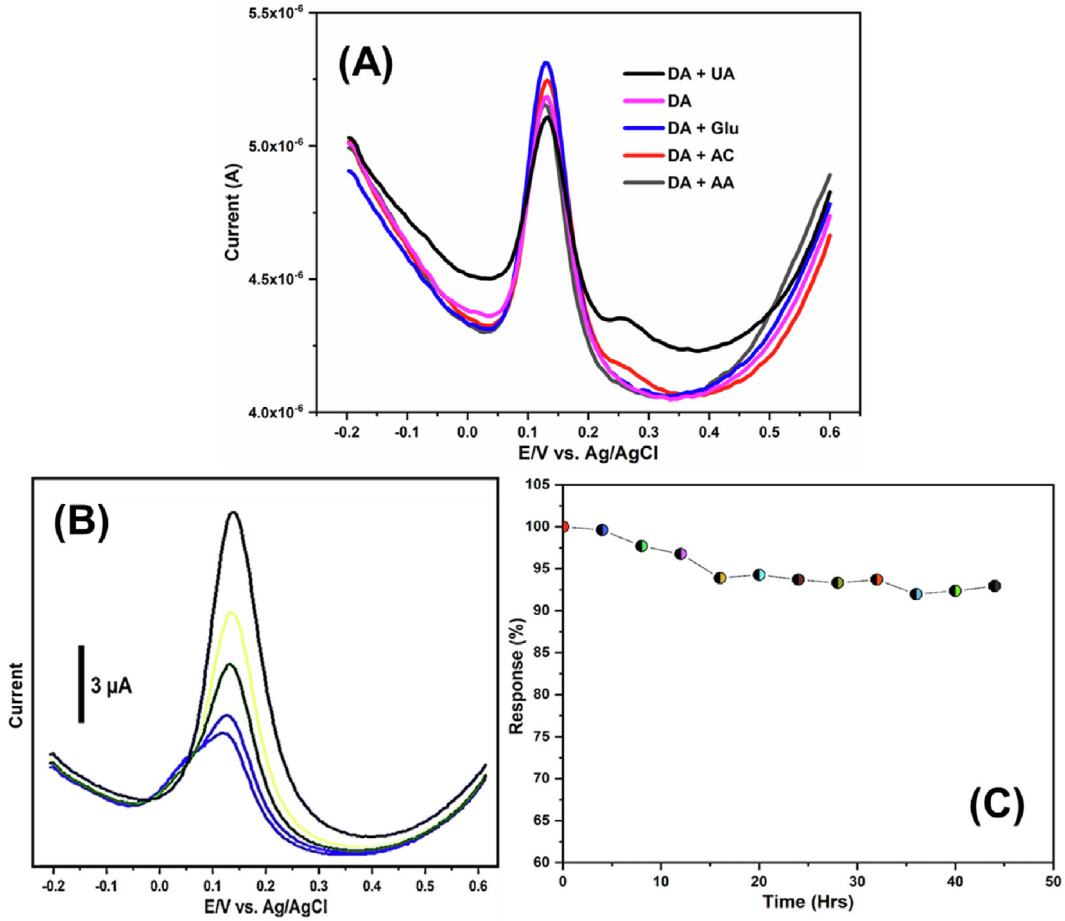

Fig. 6. A) The effect of various interfering compounds (AA, UA, Glu, and AC) on the DPV response of dopamine (DA) using the PrGO-CuS nanocomposite modified electrode. B) The DPV curves obtained for the presence of different concentrations (0.1–25 µM) of dopamine-containing BSA. C) The stability of the dopamine sensor for overtime (up to 44 h) of use.

References

[1] A.T. Smith, A.M. LaChance, S. Zeng, B. Liu, L. Sun, Synthesis, properties, and applications of graphene oxide/reduced graphene oxide and their nanocomposites, Nano Mater. Sci. 1 (2019) 31–47.

[2] V. Chabot, D. Higgins, A. Yu, X. Xiao, Z. Chen, J. Zhang, A review of graphene and graphene oxide sponge: material synthesis and applications to energy and the environment, Energy Environ. Sci. 7 (2014) 1564–1596.

[3] W. Ying, Z. Li, J. Wang, J. Li, Y. Lin, Graphene and graphene oxide: biofunctionalization and applications in biotechnology, Trends Biotechnol. 29 (2011) 205–212.

[4] G. Navarro, R. Cristina, T. Weitz, A.M. Bittner, M. Scolari, A. Mews, Ma. Burghard, K. Kern, Electronic transport properties of individual chemically reduced graphene oxide sheets, Nano Lett. 7 (2007) 3499–3503.

[5] Y. Wang, Z. Li, J. Wang, J. Li, Y. Lin, Graphene and graphene oxide: biofunctionalization and applications in biotechnology, Trends Biotechnol. 29 (2011) 205–212.

[6] B. Unnikrishnan, S. Palanisamy, S.M. Chen, A simple electrochemical approach to fabricate a glucose biosensor based on graphene–glucose oxidase biocomposite, Biosens. Bioelectron. 39 (2013) 70–75.

[7] L. Kui, G. Zhao, X. Wang, A brief review of graphene-based material synthesis and its application in environmental pollution management, Chin. Sci. Bull. 57 (2012) 1223–1234.

[8] T.S. Sreeprasad, S.M. Maliyekkal, K.P. Lisha, T. Pradeep, Reduced graphene oxide–metal/metal oxide composites: facile synthesis and application in water purification, J. Hazar. Mater. 186 (2011) 921–931.

[9] N. Karikalan, R. Karthik, S.M. Chen, C. Karuppiah, A. Elangovan, Sonochemical synthesis of sulfur doped reduced graphene oxide supported CuS nanoparticles for the non-enzymatic glucose sensor applications, Sci. Rep. 7 (2017) 2494.

[10] H.P. Cong, J.J. He, Y. Lu, S.H. Yu, Water-soluble magnetic-functionalized reduced graphene oxide sheets: in situ synthesis and magnetic resonance imaging applications, Small 6 (2010) 169–173.

[11] S. Palanisamy, S.M. Chen, R. Sarawathi, A novel nonenzymatic hydrogen peroxide sensor based on reduced graphene oxide/ZnO composite modified electrode, Sens. Actuators, B 166 (2012) 372–377.

[12] A. Pandey, A. Mukherjee, S. Chakrabarty, D. Chanda, S. Basu, Interface engineering of an RGO/MoS_2/Pd 2D heterostructure for electrocatalytic overall water splitting in alkaline medium, ACS Appl. Mater. Interfaces 11 (2019) 42094–42103.

[13] D. Thanawut, A. Karaphun, L. Wannasen, I. Kotutha, E. Swatsitang, Effect of SnS_2 concentrations on electrochemical properties of SnS_2/RGO nanocomposites synthesized by a one-pot hydrothermal method, Appl. Surf. Sci. 487 (2019) 634–646.

[14] Z. Mingjia, C. Xiang, J. Li, M. Li, N. Wu, Nanostructured carbon–metal oxide composite electrodes for supercapacitors: a review, Nanoscale 5 (2013) 72–88.

[15] K. Mujeeb, M.N. Tahir, S.F. Adil, H.U. Khan, M.R.H. Siddiqui, A.A. Al-warthan, W. Tremel, Graphene based metal and metal oxide nanocomposites: synthesis, properties and their applications, J. Mater. Chem. A 3 (2015) 18753–18808.

[16] S. Palanisamy, S. Cheemalapati, S.M. Chen, Amperometric glucose biosensor based on glucose oxidase dispersed in multiwalled carbon nanotubes/graphene oxide hybrid biocomposite, Mater. Sci. Eng., C 34 (2014) 207–213.

[17] B. Thirumalraj, S. Palanisamy, S.M. Chen, C.Y. Yang, P. Periakaruppan, B.S. Lou, Direct electrochemistry of glucose oxidase and sensing of glucose at a glassy carbon electrode modified with a reduced graphene oxide/fullerene-C60 composite, RSC Adv. 5 (2015) 77651–77657.

[18] S. Sun, P. Li, S. Liang, Z. Yang, Diversified copper sulfide ($Cu_{2-x}S$) micro-/nanostructures: a comprehensive review on synthesis, modifications and applications, Nanoscale 9 (2017) 11357–11404.

[19] X.Y. Meng, G.H. Tian, Y.J. Chen, R.T. Zhai, J. Zhou, Y.H. Shi, X.R. Cao, W. Zhou, H.G. Fu, Hierarchical CuS hollow nanospheres and their structure-enhanced visible light photocatalytic properties, CrystEngComm 15 (2013) 5144–5149.

[20] C.H. Deng, X.Q. Ge, H.M. Hu, L. Yao, C.L. Han, D.F. Zhao, Template-free and green sonochemical synthesis of hierarchically structured CuS hollow microspheres displaying excellent Fenton-like catalytic activities, CrystEngComm 16 (2014) 2738–2745.

[21] B. Hadi, M. Safaei, S. Tajik, Different Electrochemical sensors for determination of dopamine as neurotransmitter in mixed and clinical samples: a review, Anal. Bioanal. Chem. Res. 6 (2019) 81–96.

[22] B. Thirumalraj, S. Palanisamy, S.M. Chen, R. Sayee Kannan, Alumina polished glassy carbon electrode as a simple electrode for lower potential electrochemical detection of dopamine in its sub-micromolar level, Electroanalysis 28 (2016) 425–430.

[23] S. Palanisamy, S. Sakthinathan, S.M. Chen, B. Thirumalraj, T.H. Wu, B.S. Lou,

X. Liu, Preparation of β-cyclodextrin entrapped graphite composite for sensitive detection of dopamine, Carbohydr. Polym. 135 (2016) 267–273.
[24] S. Balu, S. Palanisamy, V. Velusamy, T.C.K. Yang, E.S.I. El-Shafey, Tin disulfide nanorod-graphene-β-cyclodextrin nanocomposites for sensing dopamine in rat brains and human blood serum, Mater. Sci. Eng., C 108 (2020) 110367.
[25] W. Shixin, Q. He, C. Tan, Y. Wang, H. Zhang, Graphene-based electrochemical sensors, Small 9 (2013) 1160–1172.
[26] P. Alagarsamy, G.T.S. How, T.P. See, F.S. Omar, S. Jayabal, K.Z. Kamali, N. Yusoff, A. Jamil, R. Ramaraj, S.A. John, H.N. Lim, N.M. Huang, Graphene and its nanocomposite material based electrochemical sensor platform for dopamine, RSC Adv. 4 (2014) 63296–63323.
[27] S. Palanisamy, S. Ku, S.M. Chen, Dopamine sensor based on a glassy carbon electrode modified with a reduced graphene oxide and palladium nanoparticles composite, Microchim. Acta 180 (2013) 1037–1042.
[28] W.S. Hummers, R.E. Offeman, Preparation of Graphitic Oxide, JACS 80 (1958) 1339.
[29] Sathish Kumar Ponnaiah, Periakaruppan Prakash, Saravanan Muthupandian, Ultrasonic energy-assisted in-situ synthesis of Ru^0/PANI/g-C_3N_4 nanocomposite: application for picomolar-level electrochemical detection of endocrine disruptor (Bisphenol-A) in humans and animals, Ultrason. Sonochem. 58 (2019) 104629.
[30] B. Vellaichamy, P. Periakaruppan, T. Paulmony, Evaluation of a new biosensor based on in situ synthesized PPY-Ag-PVP nanohybrid for selective detection of dopamine, J. Phys. Chem. C 121 (2017) 1118–1127.
[31] X. Yan, Y. Gu, C. Li, B. Zheng, Y. Li, T. Zhang, Z. Zhang, M. Yang, Morphology-controlled synthesis of Bi_2S_3 nanorods-reduced graphene oxide composites with high-performance for electrochemical detection of dopamine, Sens. Actuators B Chem. 257 (2018) 936–943.
[32] X. Yan, N. Lu, Y. Gu, C. Li, T. Zhang, H. Liu, Z. Zhang, S. Zhai, Catalytic activity of biomimetic model of cytochrome P450 in oxidation of dopamine, Talanta 179 (2018) 401–408.
[33] A. Ramachandran, S. Panda, S.K. Yesodha, Physiological level and selective electrochemical sensing of dopamine by a solution processable graphene and its enhanced sensing property in general, Sens. Actuators B Chem. 256 (2018) 488–497.